9-2016

On Safety Assessment of Novel Approach to Robust UAV Flight Control in Gusty Environments

Vladimir Golubev
Embry-Riddle Aeronautical University

Petr Kazarin
Embry-Riddle Aeronautical University

William MacKunis
Embry-Riddle Aeronautical University, mackuniw@erau.edu

Sherry Borener
U.S. Federal Aviation Administration

Derek Hufty
U.S. Federal Aviation Administration

ICAS 2016
30th Congress of the International Council of the Aeronautical Sciences
DCC, Daejeon, Korea ; September 25-30, 2016

ON SAFETY ASSESSEMENT OF NOVEL APPROACH TO ROBUST UAV FLIGHT CONTROL IN GUSTY ENVIRONMENTS

Vladimir Golubev*, Petr Kazarin*, William MacKunis*
*** Embry-Riddle Aeronautical University, Daytona Beach, FL, USA**
Sherry Borener, Derek Hufty****
****Federal Aviation Administration, Washington, DC, USA**

Keywords: *Robust Flight Control, UAV, Gust, Safety*

Abstract

In a follow-up to our previous study [1], the current work examines the gust-induced "cone of uncertainty" in a small unmanned aerial vehicle's (UAV) flight trajectory addressed in the context of safety assessments of UAV operations. Such analysis is a critical facet of the integration of unmanned aerial systems (UAS) into the National Airspace System (NAS), particularly in terminal airspace. The paper describes a predictive, robust feedback-loop flight control model that is applicable to various classes of UAVs and unsteady flight-path scenarios. The control design presented in this paper extends previous research results by demonstrating asymptotic (zero steady-state error) altitude regulation control in the presence of unmodeled vertical wind gust disturbances. To address the practical considerations involved in small UAV applications with limited computational resources, the proposed control method is designed with a computationally simplistic structure, without the requirement of complex calculations or function approximators in the control loop. Proof of the theoretical result is summarized, and detailed numerical simulation results are provided, which demonstrate the capability of the proposed nonlinear control method to asymptotically reject wind gust disturbances and parameter variations in the state space model. Simulation comparisons with a standard linear control method are provided for completeness.

1 Introduction

The flight trajectory of unmanned aerial vehicles (UAVs) can be significantly affected by external flow disturbances. The resulting effects present significant challenges in ensuring UAV flight safety, and addressing these challenges is of critical importance. Specifically, there is a need for control system technologies that are capable of quickly recovering from unpredictable and potentially hazardous operating conditions resulting from various phenomena such as upstream wake vortex, wind gusts, or turbulence. Based on these considerations, the focus of the current work is on the development of a nonlinear control method, which demonstrates reliable and accurate UAV trajectory regulation in the presence of unmodeled and time-varying operating conditions in addition to uncertainty in the governing UAS dynamic model.

In this paper, a robust nonlinear flight control strategy is presented, which utilizes arrays of synthetic jet actuators (SJAs) embedded in a "seamless" UAV blended wing-body design (see Figure 1) [1]. SJAs can provide enhanced maneuverability for small fixed-wing UAV applications, where the use of heavy, mechanical deflection surfaces is impractical or detrimental. The proposed control design is particularly advantageous in maintaining flight stability in the presence of a high degree of uncertainty and nonlinearity in the UAV operating conditions (e.g., flight conditions inherent in tight urban environments

and terminal zones). In addition, the proposed control method is capable of compensating for the parametric uncertainty and nonlinearity inherent in the dynamics of SJA.

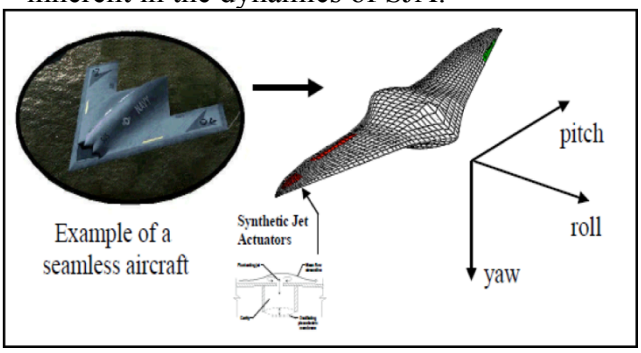

Fig. 1 – Seamless aircraft employing SJAs in a blended wing-body design.

The current work extends our recent research in [1], in which we examined the range of induced UAV flight-path (i.e., altitude) deviations resulting from the effects of various magnitudes of vertical wind gusts for UAVs operating under closed-loop control. In the current extension, the control design procedure utilizes a sliding mode control technique, which enables the closed-loop control method to achieve asymptotic regulation of the UAV altitude. Moreover, the proposed control method is capable of compensating for the uncertainty in the SJA actuator dynamics. A brief summary of the control design procedure is presented, and numerical simulation results are provided, which demonstrate the improved performance of the proposed control design over a standard linear control method.

2 Mathematical Model

This section describes the mathematical model utilized to develop our nonlinear control method. The subsequently provided numerical simulation results were obtained using the mathematical models presented in this section for the UAV, SJA actuator dynamics, and wind gusts.

The UAV dynamic model under consideration in this paper is assumed to contain parametric model uncertainty in addition to unmodeled, time-varying nonlinearities. Specifically, the UAV system can be modeled via a quasi-linear state space system as [4], [5], [6], [7], [8], [9], [10]

$$\dot{x} = Ax + Bu + f\left(x,t\right) \qquad (1)$$

where $A \in \circ^{n\times n}$ represents a constant, uncertain state matrix; and $B \in \circ^{n\times m}$ denotes an uncertain input gain matrix. In Equation (1), the state vector

$x\left(t\right) \triangleq \left[v\left(t\right) \quad w\left(t\right) \quad q\left(t\right) \quad \theta\left(t\right) \quad h\left(t\right)\right]^T \in \mathbf{R}^5$, where the state elements include vertical and horizontal components of velocity $v(t)$ and $w(t)$, pitch rate $q(t)$, pitch angle $\theta(t)$, and altitude $h(t)$[3], [11]. In (1), $f\left(x,t\right)$ denotes a general, unknown nonlinear disturbance. For example, $f\left(x,t\right)$ could represent exogenous disturbances (e.g., due to wind gusts) or nonlinearities not captured in the linearized dynamic model, for example. Also in (1), the control input term $u\left(t\right) \triangleq \left[\delta_e\left(t\right) \quad \delta_t\left(t\right)\right]^T \in \circ^{m}$, where $\delta_e\left(t\right) \in \circ^{m-1}$ denotes the elevator control deflection angle; and $\delta_t\left(t\right) \in \circ$ is the throttle input. In our SJA-based UAV control application, the (virtual) elevator deflection angle input $\delta_e\left(t\right)$ is generated by an array consisting of $m-1$ SJAs. Thus, the virtual elevator deflection angle input can be expressed as

$$\delta_e\left(t\right) \triangleq \left[u_1\left(t\right) \quad u_2\left(t\right) \quad \mathrm{L} \quad u_{m-1}\left(t\right)\right]^T \qquad (2)$$

where represents the virtual surface deflection due to the array of SJAs. Based on empirical studies, the dynamics of the SJA can be modeled as [6], [7], [8], [12]

$$u_i\left(t\right) = \theta_{2i}^* - \frac{\theta_{1i}^*}{V_i\left(t\right)}, \quad i = 1,2,\mathrm{K}\ ,m-1 \qquad (3)$$

where $V_i\left(t\right) = A_{ppi}^2\left(t\right) \in \circ$ denotes the peak-to-peak voltage acting on the i^{th} SJA array; and θ_{1i}^*, $\theta_{2i}^* \in \circ$ are uncertain constant physical parameters. One of the control design challenges is that the control terms in $u_i\left(t\right)$

depend nonlinearly on the voltage signal $V_i(t)$ and contain parametric uncertainty due to θ_{1i}^* and θ_{2i}^*. This challenge will be mitigated using a robust nonlinear control technique.

3 Wind Gust Model

This section describes the mathematical model for a vertical discrete wind gust as defined in Federal Aviation Regulations (FAR) [13]. The FAR wind gust model is used in the subsequent numerical simulation code to test the capability of the proposed control method to reliably regulate a UAV flight trajectory in the presence of various magnitudes of wind gusts.

An example of a bounded external disturbance, which could be represented by $f(x,t)$ in Equation (1), is a discrete vertical gust. The formula given in the FAR defines such a bounded nonlinearity in the longitudinal axis as [13]

$$f(x,t)=\begin{bmatrix}-11.1\\ 7.2\\ 37.4\\ 0\end{bmatrix}\frac{1}{V_0}\left\{\frac{U_{ds}}{2}\left[1-\cos\left(\frac{\pi s}{H}\right)\right]\right\}, \quad (4)$$

where H denotes the distance (between 35 feet and 350 feet) along the aircraft flight path for the gust to reach its peak velocity, V_0 is the forward velocity of the aircraft when it enters the gust, $s\in[0,2H]$ represents the distance penetrated into the gust (i.e., $s=\int_{t_1}^{t_2}V(t)dt$, where $V(t)$ is the forward velocity element of the state vector x), and U_{ds} is the design gust velocity as specified in [13]. This FAR formulation is intended to be used to evaluate both vertical and lateral gust loads, so a similar representation can be developed for the lateral dynamics.

4 Control Objective

The control objective is to force the UAV altitude and pitch rate (i.e., $h(t)$ and $q(t)$) to track a given desired constant value in spite of model uncertainty and external disturbances. To quantify the control objective, the trajectory regulation error $e(t)\in\mathbf{R}^2$ and auxiliary regulation error $r(t)\triangleq[r_q(t)\quad r_h(t)]^T\in\mathbf{R}^2$ are defined as

$$e(t)=\begin{bmatrix}h(t)-h_d\\ \theta(t)\end{bmatrix} \quad (5)$$

$$r(t)=\begin{bmatrix}r_h(t)\\ r_q(t)\end{bmatrix}=\begin{bmatrix}\dot{h}(t)+\alpha_1(h(t)-h_d)\\ q(t)+\alpha_2\theta(t)\end{bmatrix}. \quad (6)$$

In Equation (6), α_1, $\alpha_2\in\mathbf{R}$ denote positive, constant control gains.

Thus, the trajectory regulation control objective can be stated mathematically as $\|e(t)\|\to 0$, where $\|\cdot\|$ denotes the standard Euclidean norm of the vector argument. Note that, based on the auxiliary regulation error definitions in Equation (6), $\|r(t)\|\to 0\Rightarrow\|e(t)\|\to 0$.

Remark 1: The regulation error and auxiliary errors defined in Equations (5) and (6) are a key aspect of the contribution presented here. The definitions of the auxiliary regulation errors enable us to recast the dynamic model in Equation (1) in a form that is amenable to altitude and pitch angle regulation control. Indeed, it can be seen that differentiation of $r(t)$ produces a set of equations that render the altitude and pitch angle states $h(t)$ and $\theta(t)$ fully controllable through the elevator deflection and throttle inputs $\delta_e(t)$ and $\delta_t(t)$. Thus, the auxiliary error terms $r_h(t)$ and $r_q(t)$ can be viewed as sliding surfaces, which enable us to prove our altitude and pitch angle regulation result.

5 Robust Controller Development

A contribution of the control method presented in this paper is the capability of the proposed control strategy to asymptotically compensate for the control input nonlinearity and parametric uncertainty in the SJA dynamic model in Equation (3). To achieve this, a robust inverse structure for $V_i(t)$, $i=1,...,m-1$ will be utilized, which contains constant feedforward best-guess estimates of the uncertain parameters θ_{1i}^* and θ_{2i}^*. The robust inverse that compensates for the uncertain jet array nonlinearities in (3) can be expressed as [14]

$$V_i(t)=\frac{\hat{\theta}_{1i}}{\hat{\theta}_{2i}-u_{di}(t)},\quad i=1,...,m-1 \qquad (7)$$

where $\hat{\theta}_{1i}$, $\hat{\theta}_{2i}\in°^{+}$ are constant feedforward estimates of θ_{1i}^* and θ_{2i}^*, respectively; and $u_{di}(t)\in°$ for $i=1,...,m-1$ are subsequently defined auxiliary control signals. *Note that the robust-inverse structure in (7) is only required for the virtual elevator deflection angle control inputs in* $\delta_e(t)$.

Remark 2: Preliminary results show that the auxiliary control signal $u_{di}(t)$ in (7) can be designed to achieve asymptotic trajectory regulation control and disturbance rejection for the uncertain dynamic model in (1) - (3) over a wide range of feedforward estimates $\hat{\theta}_{ji}\neq\theta_{ji}^*$, *for* $i=1,...,m-1$ *and* $j=1,2$.

Remark 3: The controller design presented in this paper is valid for systems in the form of Equations (1) - (3), where the total number of control inputs (i.e., the throttle and the SJA arrays) is greater than or equal to the number of states to be controlled (i.e., the m ≥ n case). For the case where m > n, the following control design can easily be modified using the matrix pseudoinverse definition, for example. The underactuated case where m < n would require a specialized design methodology and is not addressed in the current result. The following control design and subsequent simulation results are based on the case where m = n = 2, without loss of generality.

Based on the original dynamic model in (1) - (3) and the auxiliary regulation error definitions in (6), the auxiliary control term $u_d(t)$ is designed as

$$u_d(t)=\hat{\Omega}^{-1}\left(\begin{bmatrix}k_1 r_h\\ k_2 r_q\end{bmatrix}+\begin{bmatrix}\beta_1 sign(10r_h)\\ \beta_2 sign(10r_q)\end{bmatrix}\right) \qquad (8)$$

where $\hat{\Omega}\in°^{2\times2}$ denotes a constant auxiliary matrix containing estimates of the uncertain SJA parameters, and $[g]^{-1}$ denotes the inverse of a matrix. The feedback control gains (i.e., amplifiers) β_1, β_2, k_1 and k_2 can be tuned to adjust the closed-loop trajectory regulation response to achieve the desired system performance (e.g., to achieve a faster response time). *It should again be noted that the robust-inverse structure in (7) only applies to the elevator deflection input* $\delta_e(t)$*; the thrust control input* $\delta_t(t)$ *directly implements the corresponding control vector element in equation (8)*

6 Stability Analysis

Theorem 1: The robust nonlinear control law given by Equations (7) and (8) ensures asymptotic trajectory tracking in the sense that

$$\|e(t)\|\to 0,\quad \text{as}\quad t\to\infty \qquad (9)$$

provided the control gains k_1 and k_2 introduced in (8) are selected sufficiently large, and β_1 and β_2 are selected based on the known upper bounds on the disturbance (i.e., the known maximum velocity and acceleration of the wind gust).

Proof: A straightforward Lyapunov-based stability analysis can be utilized to prove Theorem 1 and is omitted here to avoid distraction from the main contribution of the current result. Details of the proof are similar to those provided in our recent results in [1],[14] and are omitted here for brevity.

7 Test Study

A numerical simulation study was conducted to test the performance of the proposed controller. The simulation code was developed using the Matlab/Simulink software package (version R2014b). The simulation is based on the aircraft state space system in (1) - (3), where the numerical values for the state matrix A and input gain matrix B are based on the linearized model for a fixed wing medium sized UAV [11], [3]

8 Numerical Simulation

The flight dynamic model used in the numerical simulation is given by Equation (1), where the nominal values for the state and input matrices are [3], [11]

$$A = \begin{pmatrix} -0.0844 & 0.4354 & -4.3589 & -9.7483 & 0 \\ -0.2920 & -1.8188 & 39.7431 & -1.0682 & 0 \\ 0.0313 & -0.3089 & -2.3089 & -2.3953 & 0 \\ 0 & 0 & 1 & 0 & 0 \\ 0 & -1 & 0 & 47 & 0 \end{pmatrix}$$

$$B = \begin{bmatrix} -0.0494 & 144.8262 \\ -3.2438 & 0 \\ 8.6497 & -7.2413 \\ 0 & 0 \\ 0 & 0 \end{bmatrix}$$

To test the capability of the control law to compensate for parameter variations, an additive sinusoidal variation in the elements of A was simulated having an amplitude of 1.5 and a frequency of 1 rad/s.

In order to develop a realistic demonstration of the performance of the proposed nonlinear UAV trajectory regulation controller, the nonlinear disturbance term $f(x,t)$ used in the simulation is based on the FAR discrete vertical gust model as described in (4) [13], where $H = 15.24$ m, and $V_0 = 47\ m/s$, (cruise velocity). Since the state vector is this case is defined as $x(t) \triangleq [v(t) \quad w(t) \quad q(t) \quad \theta(t) \quad h(t)]^T$, the constant gain parameters of simulated model were modified slightly from (4). The remainder of the additive disturbances in $f(x,t)$ represents nonlinearities not captured in the linearized state space model (e.g., due to small angle assumptions). The controlled states were initialized to the trim conditions of $h(0) = 500$ m, $\theta(0) = 0$ deg and $q(0) = 0$ deg/s; and all control inputs were initialized to zero for the simulation.

The SJA actuator dynamic model uses the following well-accepted, empirically determined values for the constant parameters θ_1^* and θ_2^* (see [6] – [8]):

$$\theta_1^* = 33.33, \quad \theta_2^* = 15 \tag{10}$$

Remark 4: The values used in the simulation for the parameters θ_1^* and θ_2^* are used to generate the SJA dynamic model only. The parameters are assumed to be uncertain, and are not used in the feedback control law. Our preliminary results show that the robust control method presented here is capable of achieving asymptotic (zero steady-state error) tracking control of a SJA-based UAV system when the constant estimates $\hat{\theta}_1$ and $\hat{\theta}_2$ differ by as much as 10 % from the actual values θ_1^* and θ_2^*.

9 Results

The objectives for the regulation control task are to track pitch rate and altitude commands. Table I provides a summary of the maximum flight path deviations demonstrated in the simulation. The results summarized in Table I illustrate the improved capability of our nonlinear control method over a standard linear controller for the trajectory regulation objective tested here.

The control gains selected for the nonlinear control law in the simulation are (see Equation (8)):

$$k_1 = 235, \quad k_2 = 0.1, \beta_1 = 0.2, \quad \beta_2 = 0.001 \tag{11}$$

The gain values in (11) were selected manually to achieve desirable closed-loop regulation performance.

To provide a comparison with a standard linear control method, a pole-placement

technique (using the Matlab 'place' function) was utilized to calculate a full-state feedback gain matrix, K, such that the closed-loop system's poles are placed at $P = \begin{bmatrix} -1 & -2 & -2.5 & -2.1 & -4 & -1 \end{bmatrix}^T \in \mathbf{R}^6$. Note that the state vector for the transformed system includes the auxiliary state variables $r_h(t)$ and $r_q(t)$ so that the control-oriented model contains six states. The A and B matrices were modified slightly in the transformed model for the simulation to ensure that the closed-loop system is consistent with the original dynamic model in (1).

Using this method, the linear full-state feedback control law obtained for the simulation is

$$u_d(t) = -Kx \qquad (12)$$

where the gain matrix K is explicitly given as

$$K = \begin{bmatrix} 0.0100 & 0.1243 & -0.7635 & 0.3312 & -0.0205 & 0.0528 \\ 0.0137 & 0.1331 & -1.8525 & 0.8509 & -0.0308 & 0.0742 \end{bmatrix}$$

Figures 2 – 13 show the detailed time evolution of the wind gusts and flight trajectories during closed-loop linear and nonlinear controller operation for three test cases with wind gusts of 10 m/s, 20 m/s, and 30 m/s.

Figure 2 – 5 show the gust velocity, followed by the closed-loop trajectory tracking results in the presence of a 10 m/s FAR wind gust. In all four of the following test cases, the objective is for the aircraft to maintain straight level flight at an altitude of 500 m and 0 deg/s pitch rate, while minimizing the pitch angle deviation. Fig.2 shows the pitch rate, Figure 4 shows the pitch angle, and Fig.4 shows the altitude deviation under closed-loop control for the 10 m/s wind gust scenario. The results in this test case demonstrate that the nonlinear control law can more reliably compensate for the wind gust disturbance and accurately track the reference trajectory within safety constraints. Specifically, the maximum altitude deviation remained within a 2.2 m magnitude for nonlinear case and 5.5 m for linear case, both of which are well within the recently reduced vertical separation minimum of 500 feet (152 m), as specified in [13]. As for pitch rate and pitch angle deviations, it can be seen that nonlinear control law compensates for the gust disturbance significantly more effectively than the linear control law.

Table I: Summary of flight path deviations obtained from numerical simulations.

Gust Speed	Max Altitude Deviation (Linear/ Nonlinear)	Max Pitch Angle Deviation (Linear/ Nonlinear)	Max Pitch Rate Deviation (Linear/ Nonlinear)
10 m/s	5.5 m/ 2.2 m	24.7 deg/ 3 deg	16 deg/s/ 6 deg/s
20 m/s	11 m/ 4.5 m	49 deg/ 4 deg	33 deg/s/ 11 deg/s
30 m/s	16 m/ 7 m	73 deg/ 7 deg	48 deg/s/ 15 deg/s

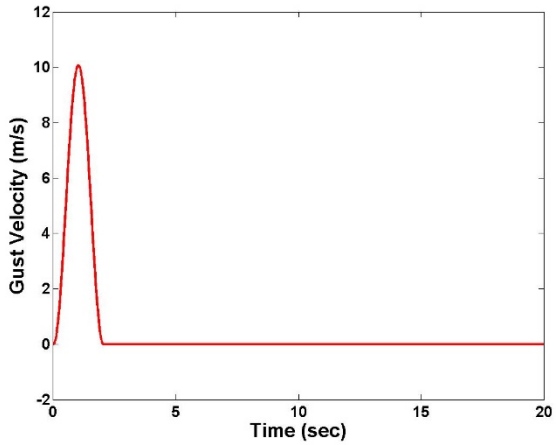

Fig. 1 – Vertical gust velocity (10 m/s)

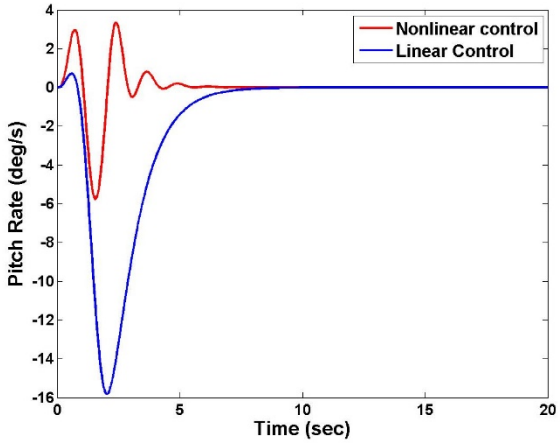

Fig.2 – Pitch rate deviation during closed-loop controller operation for a 10 m/s gust.

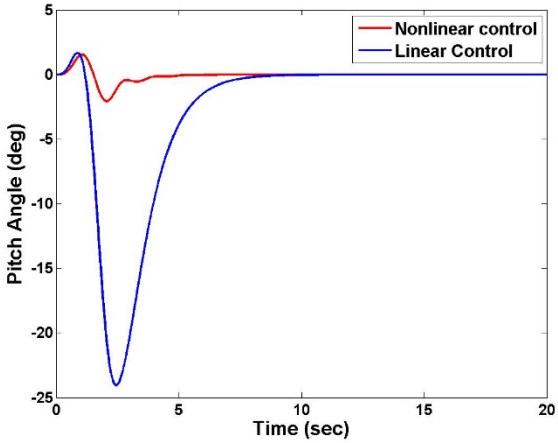

Fig.3 – Pitch angle deviation during closed-loop controller operation for a 10 m/s gust.

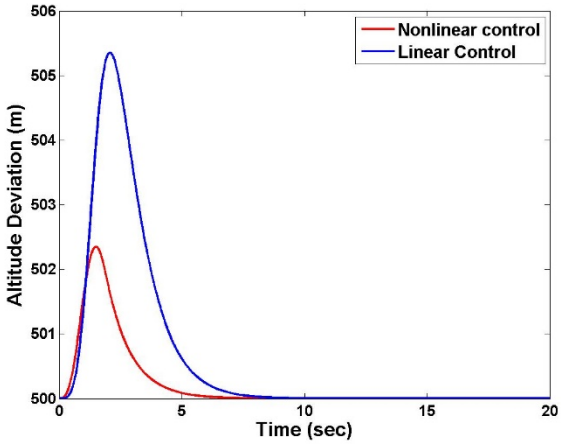

Fig.4 – Altitude deviation during closed-loop controller operation for a 10 m/s gust.

Figures 6 – 9 show the closed-loop tracking control results in the presence of a 20 m/s wind gust, and Figure 10 – 13 show the results in the presence of a 30 m/s wind gust. In all cases, the results demonstrate the improved trajectory regulation performance of the nonlinear control method in comparison to linear controller. Altitude, pitch rate and pitch angle deviations are much smaller using the nonlinear control method.

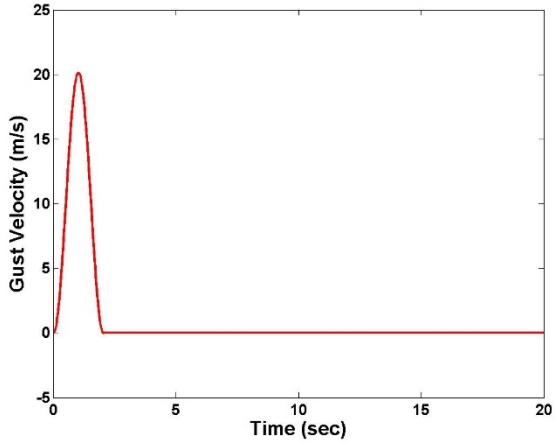

Fig.5 – Vertical gust velocity (20 m/s)

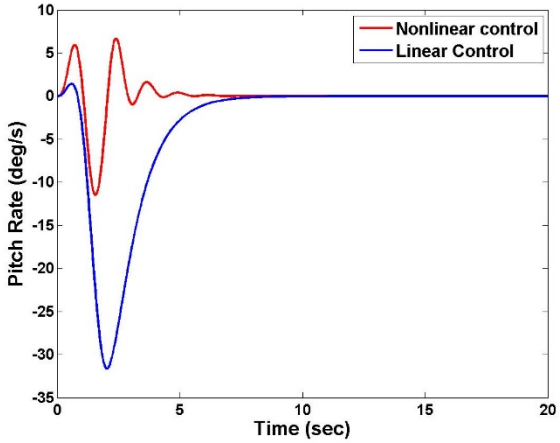

Fig.6 – Pitch rate deviation during closed-loop controller operation for a 20 m/s gust

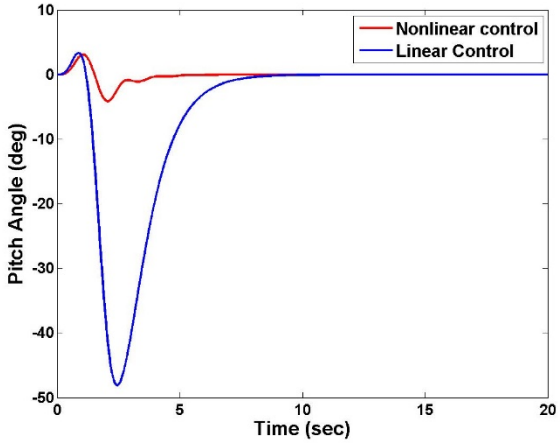

Fig.7 – Pitch angle deviation during closed-loop controller operation for a 20 m/s gust

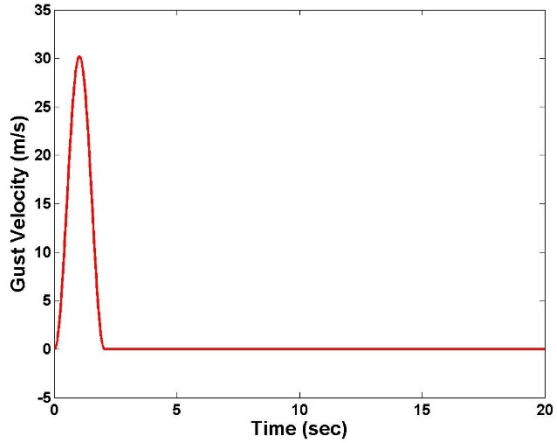

Fig.8– Vertical gust velocity (30 m/s)

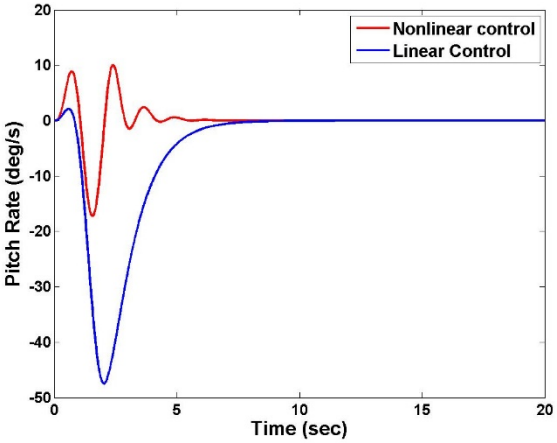

Fig.9 – Pitch rate deviation during closed-loop controller operation for a 30 m/s gust.

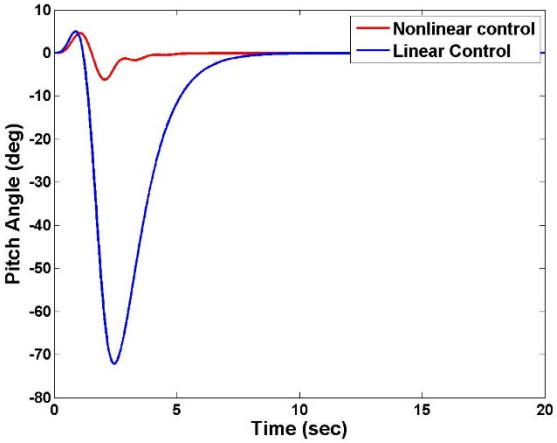

Fig.11– Pitch angle deviation during closed-loop controller operation for a 30 m/s gust

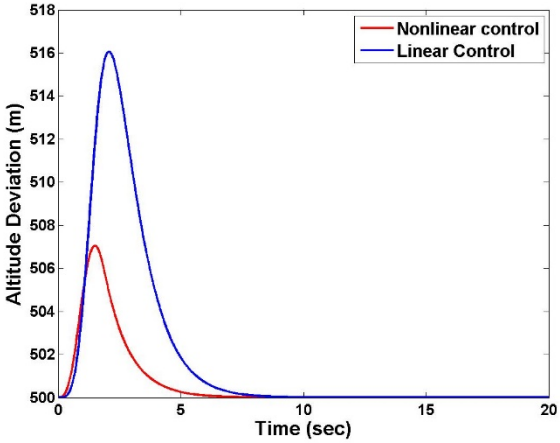

Fig.13 – Altitude deviation during closed-loop controller operation for a 30 m/s gust

In Figures 14 - 16 the closed-loop results in the presence of a 30 m/s gust are presented, where the state matrix A includes parameter variations. The results clearly demonstrate that the linear controller cannot provide stability in this case, while nonlinear control law compensates for the disturbances and parameter variations while keeping the system within acceptable limits.

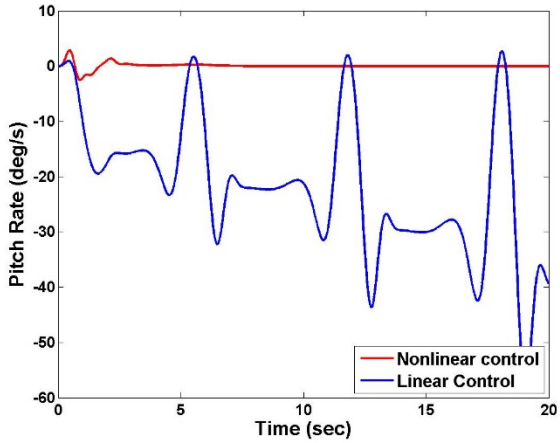

Fig.14 – Pitch rate deviation during state matrix elements variation and a presence of 30 m/s gust

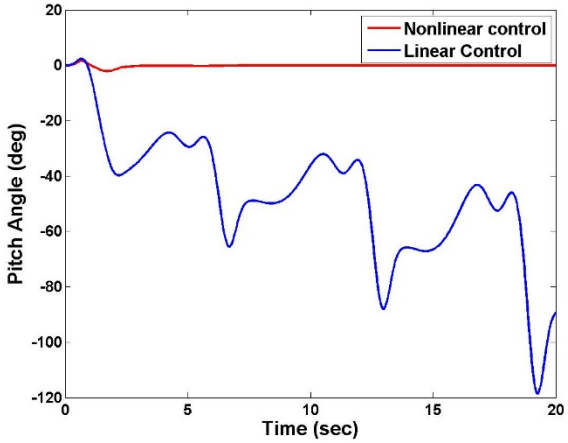

Fig.15 – Pitch angle deviation during state matrix elements variation and a presence of 30 m/s gust

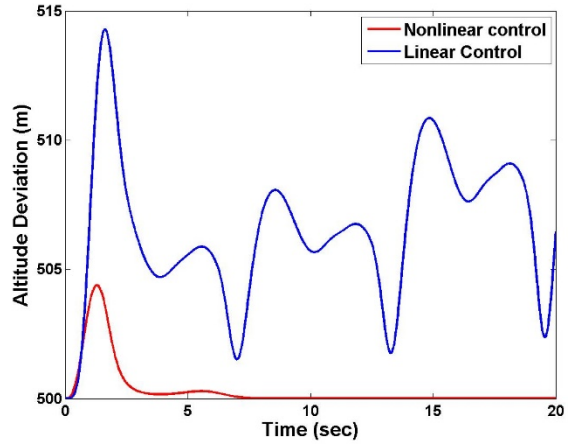

Fig.16 – Altitude deviation during state matrix elements variation and a presence of 30 m/s gust

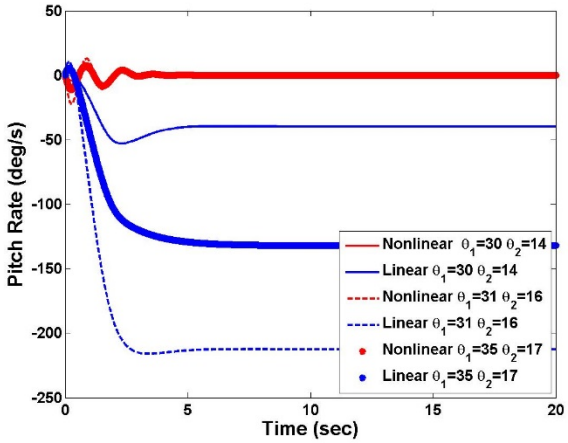

Fig.17 Pitch rate deviation during SJA parameters variation

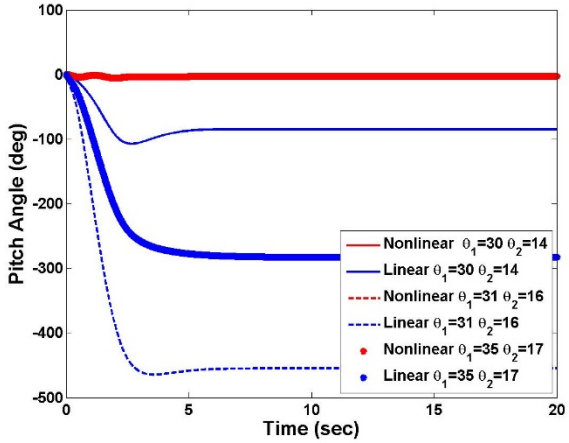

Fig.18 Pitch angle deviation during SJA parameters variation

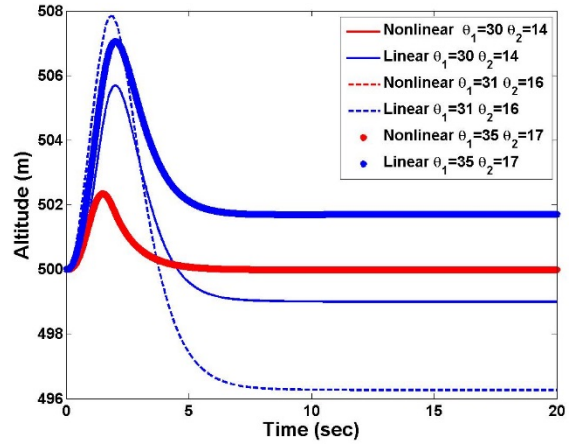

Fig.19 Altitude deviation during SJA parameters variation

Figures 17-19 reveal the closed-loop trajectory regulation results under uncertainty in the θ_1^* *and* θ_2^* SJA parameters. Deviation of up to 10% were tested, and the results show that the nonlinear control method compensates for the parameter deviations, while the linear control method does not. The specific values for the parameter deviations are provided in the legends of Figures 17 – 19.

Conclusions

A nonlinear UAV regulation control method is presented, which can be proven to asymptotically regulate pitch angle and altitude in the presence of extreme wind gust disturbances. Moreover, the control method presented can be proven to achieve reliable results in the presence of significant uncertainty in the aircraft and SJA actuator dynamic model. Detailed numerical simulation results are

provided to demonstrate the performance of the proposed nonlinear control law. To provide a basis for comparison, the same control objective is simulated using a standard linear control law. It is shown that the nonlinear control method compensates for the wind gust disturbances significantly more effectively than the linear controller. Moreover, parameter variations in the state space model were introduced in the simulation. The results clearly show that the nonlinear control design outperforms the linear control method for the simulated trajectory regulation objective under all tested levels of uncertainty, parameter variations, and wind gust disturbances.

References

[1] V.V. Golubev, W. MacKunis, 2014. "On UAV Robust Nonlinear Control in Presence of Parametric Uncertainties," *ICAS 2014-0731*, *29th Congress of the International Council of the Aeronautical Sciences*, St. Petersburg, Russia, September 2014.

[2] N. Ramos Pedroza, W. MacKunis, V.V. Golubev, 2014. "Robust nonlinear regulation of limit cycle oscillations in UAVs using synthetic jet actuators, *Robotics*, Vol. 3, pp. 330-348.

[3] K. Natesan, D.W.Gu, I.Postlethwaite, 2007, "Design of static H_∞ linear parameter varying controllers for unmanned aircraft" *JOURNAL OF GUIDANCE, CONTROL, AND DYNAMICS*, Vol. 30, No. 6, November–December 2007

[4] A. A. Tchieu, A. T. Kutay, J. A. Muse, A. J. Calise, and A. Leonard, 2008. "Validation of a low-order model for closed-loop flow control enable flight," *AIAA* Paper 2008-3863.

[5] R. Nelson, 1998. Flight Stability and Automatic Control, 2nd ed. New York:McGraw-Hill.

[6] D. Deb, G. Tao, J. O. Burkholder, and D. R. Smith, "An adaptive inverse control scheme for a synthetic jet actuator model," in *American Control Conference*, June 2005, pp. 2646-2651.

[7] --, "Adaptive compensation control of synthetic jet actuator arrays for airfoil virtual shaping," *Journal of Aircraft*, vol. 44, no. 2, pp. 616 - 626, Mar.-Apr. 2007.

[8] --, "Adaptive synthetic jet actuator compensation for a nonlinear aircraft model at low angles of attack," *IEEE Transactions on Control Systems Technology*, vol. 16, no. 5, pp. 983-995, Sept. 2008.

[9] . T. Mondschein, G. Tao, and J. O. Burkholder, "Adaptive actuator nonlinearity compensation and disturbance rejection with an aircraft application," in *American Control Conference*, June-July 20 1 1, pp.295 1-2956.

[10] C. Singhal, G. Tao, and 1. O. Burkholder, "Neural network-based compensation of synthetic jet actuator nonlinearities for aircraft flight control," in *AIAA Guidance, Navigation, and Control Conf*, Chicago,IL,2009.

[11] N. Kumar and S. Jain, "Identification, modeling and control of unmanned aerial vehicles," in *International Journal of Advanced Science and Technology*. Vol.67 (2014), pp.1-10. http://dx.doi.org/10.14257/ijast.2014.67.01

[12] D. Deb, G. Tao, J. O. Burkholder, and D. R. Smith,, "Adaptive synthetic jet actuator compensation for a nonlineartailless aircraft model at low angles of attack," in *American Control Conference*, June 2006.

[13] Department of Transportation, "Airworthiness standards: transport category airplanes," in *Federal Aviation Regulations*, Washington, DC, 2015.

[14] W. MacKunis, S. Subramanian, S. Mehta, C. Ton, J. W. Curtis, and M. Reyhanoglu. "Robust nonlinear aircraft tracking control using synthetic jet actuators" *IEEE 52nd Annual Conference on Decision and Control (CDC)* Jan. 2013: 220-225.

10 Contact Author Email Address

Vladimir.Golubev@erau.edu

Copyright Statement